Hypothetical Efficiency of Electrical to Mechanical Energy Transfer during Individual Stochastic Molecular Switching Events

Amanda M. Larson[1§], Tedros A. Balema[1§], Percy Zahl[2], Alex C. Schilling[1], Dario J. Stacchiola[2], and E. Charles H. Sykes[1*]

[1] Department of Chemistry, Tufts University, Medford, Massachusetts 02155, United States

[2] Center for Functional Nanomaterials, Brookhaven National Laboratory, Upton, New York 11973, United States

§ These authors contributed equally

* Corresponding author: charles.sykes@tufts.edu

Abstract

There are now many examples of single molecule rotors, motors and switches in the literature that, when driven by photons, electrons or chemical reactions, exhibit well defined motions. As a step towards using these single molecule devices to perform useful functions one must understand how they interact with their environment and quantify their ability to perform work on it. Using a single molecule rotary switch we examine the transfer of electrical energy, delivered *via* electron tunneling, to mechanical motion and measure the forces the switch experiences with a non-contact q-plus atomic force microscope. Action spectra reveal that the molecular switch has two stable states and can be excited resonantly between them at a bias of 100 mV *via* a one-electron inelastic tunneling process which corresponds to an energy input of 16 zepto Joules. While the electrically induced switching events are stochastic and no net work is

done on the cantilever, by measuring the forces between the molecular switch and the AFM cantilever we can derive the maximum hypothetical work the switch could perform during a single switching event which is ~55 meV, equal to 8.9 zepto Joules which translates to a hypothetical efficiency ~55% per individual inelastic tunneling electron induced switching event. When co considering the total electrical energy input this drops to $1x10^{-7}$ % due to elastic tunneling events that dominate the tunneling current. However, this approach constitutes a general method for quantifying and comparing the energy input and output of molecular-mechanical devices.

Keywords: molecular rotor, AFM, STM, Cu(111), Ullmann coupling, qPlus

Synthetic molecular machines are a rapidly advancing field in which motors, actuators and switches driven by chemical, optical and electrical energy have been demonstrated.[1–10] While the complexity of these systems continues to increase, and their mechanism of operation becomes more deeply understood, a major challenge is to connect to these molecular devices and measure the forces they exert on their environment. Some seminal examples of ensembles of molecular motors moving macroscopic objects like water droplets up an incline[11] or small glass bars exist,[12] but a direct measurement of energy transfer within individual molecule devices is lacking.

In recent years non-contact atomic force microscopy (NC-AFM) with metal tips functionalized with closed-shell molecules like CO have revolutionized the field of molecular imaging.[13–23] These well-defined, fairly inert probe tips have enabled the internal structure of organic molecules on surfaces to be imaged while probing relatively large tip-molecule forces at very close proximity *(into the Pauli exclusion/repulsion regime)* without the probe tip itself being destroyed.[13,14,24–26] This imaging technique that can resolve submolecular features has been used to characterize a wide variety of organic molecules on metallic or insulating surfaces.[13,14,16,17,27]

It has also been used to quantify the forces needed to manipulate molecular confirmations on surfaces.[28–31] The work of Lotze *et al.* in which the authors report the transfer of energy from the stochastic motion of surface-adsorbed H_2 molecules to the oscillation of the AFM cantilever itself is of particular relevance to this study.[32] Herein we describe an approach using a combination of scanning tunneling microscopy (STM) Action Spectroscopy, and non-contact atomic force microscopy (nc-AFM) that enables the electrical energy input and the forces between the molecular switch and the AFM tip to be measured. To perform reliable single molecule measurements, one must consider variability introduced by the local environment on the molecular properties. In this sense crystalline systems, with their regular repeating unit cells, offer an ideal testbed in which the molecules are in identical environments. We focus on 2D crystalline molecular rotor arrays that exhibit discreet switching events that can be triggered by a STM tip.

Results and Discussion

Figure 1 shows both AFM and STM images of the 2D molecular rotary switch arrays and demonstrates how single molecular rotor switching is observed. Panels A-C show representative images in frequency shift, AFM tip tunneling current, and STM modes of the 2D arrays respectively. We have previously studied the structures of these 2D molecular rotor arrays.[33–36] Briefly, when 4-bromo-1-ethyl-2-fluorobenzene is deposited on a Cu(111) surface and annealed to 260 K the C-Br bond is broken and organometallic intermediates of the Ullmann coupling reaction[37] form on the surface as shown in Figure 1E. These organometallic intermediates spontaneously self-assemble into a variety of 2D crystal structures on the Cu(111) surface. The structure and dimensions of the ordered molecular rotor arrays dictate the correlated switching

properties of the internal submolecular rotor units.[34] The structure of interest to this study is shown in Figure 1 in which the molecules adopt a pseudo-herringbone type packing.

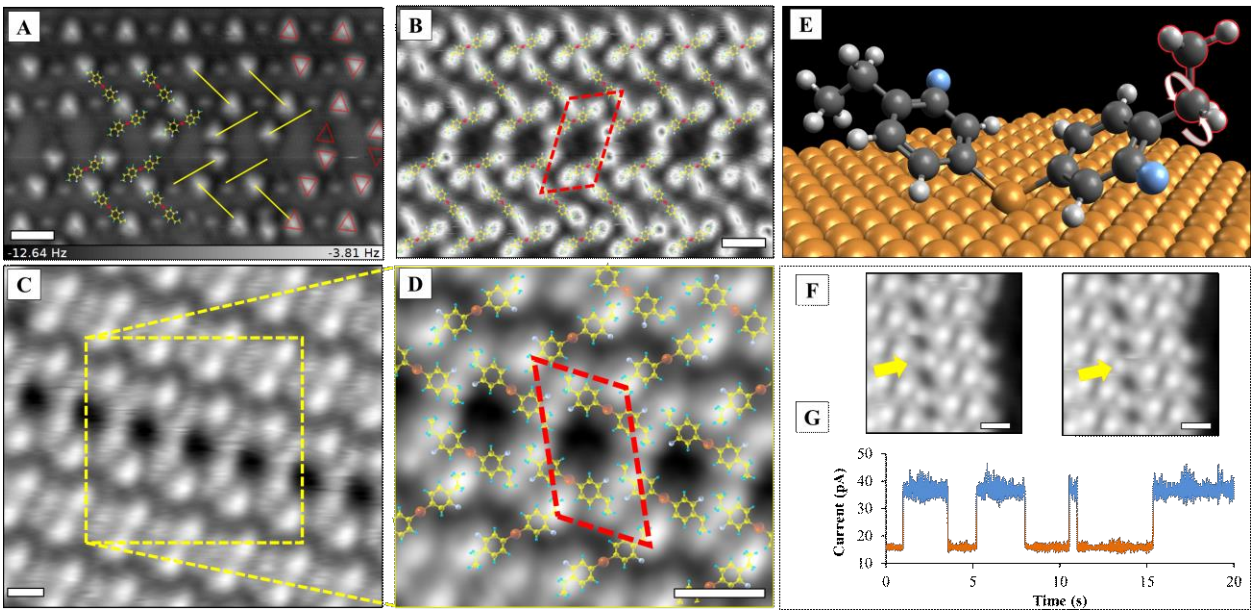

Fig. 1 (A) nc-AFM image at 5 K of a 2D domain of 4-bromo-1-ethyl-2-fluorobenzene Ullmann coupling intermediates. Molecular models are overlaid along with yellow lines to indicate the orientations of the organometallic intermediates. Red triangles indicate the orientation of the ethyl rotor tail of the molecules. Imaging conditions: 100 mV, constant height, Br terminated tip. **(B)** Tunneling current image from AFM measurement in 1A with molecular models and the 1D unit cell of the active row highlighted in red. Imaging conditions: 100 mV, constant height. **(C)** Topographic 5 K STM image of an active swicthing row of the 4-bromo-1-ethyl-2-fluorobenzene intermediates. Imaging conditions: 160 mV, 20 pA. **(D)** Close-up of the area in STM image 1C heighted by the yellow square, with molecular models overlaid with the 1D unit cell of the active row highlighted in red. **(E)** Molecular model of the 4-bromo-1-ethyl-2-fluorobenzene Ullmann coupling intermediate, with an ethyl rotor highlighted in red and the axis of rotation indicated with white arrows. **(F)** STM images of active rows of 4-bromo-1-ethyl-2-fluorobenzene intermediates before (left) and after (right) an I(t) measurement in which the ethyl switch transitions from down to up, where the yellow arrow indicates the placement of the STM tip. **(G)** Accompanying $I(t)$ tunneling current *vs.* time trace with

two tunneling current levels highlighted that correspond to the two stable orientations of the ethyl rotor. Orange corresponds to the rotor oriented down and blue refers to the rotor oriented up. Imaging conditions: 100 mV, 5 pA. Excitation conditions: 110 mV, 80 pA. Scale Bars: 1 nm.

In the 4-bromo-1-ethyl-2-fluorobenzene Ullmann coupling intermediate each phenyl group is bonded to a central Cu atom and tilted off the surface ~30 degrees as seen in Figure 1E.[38–40] The ethyl rotors attached to the highest side of the phenyl rings have preferred orientations pointed either away from, or towards the surface.[34] The image in panel A clearly shows the rotor groups that are pointed up as AFM mode is most sensitive to the topographic height of surface features. However, rotary switching can be clearly seen in both AFM and STM modes (panels A-D). For example, panel F shows STM images before and after a single rotor switching event in which a rotor initially oriented in the down position is switched up. Panel G shows the corresponding tunneling current *vs.* time trace where the tunneling current starts low and ends high, consistent with a down to up switching event. In these particular 2D array structures we only observe rotary switching associated with the molecules located along the domain boundaries.

Figure 2 shows a summary of STM based Action Spectroscopy[41] and power law fits[42] that enable us to quantify the electrical energy needed to switch the ethyl rotor groups between their two stable states. Panel A shows Action Spectroscopy in which the rate of a switching event is plotted against tip-sample bias difference, and hence the energy of the tunneling electrons at a set tunneling current. One can see from the lower log plot that the molecular rotor switching rate increases rapidly as the voltage approaches 100 mV. The upper Action Spectrum shows that there is a local maximum in the switching rate at both +102 ± 5 mV and −97 ± 4 mV. The fact that the Action Spectrum is symmetric about zero implies that switching of the molecule in this 2D structure occurs *via* an inelastic electron tunneling process because the electrons excite the

mode regardless of their direction of flow. To further investigate the mechanism of electrical activation of the molecular switches we measured the switching rate as a function of tunneling current, at and above the threshold onset voltage (Figure 2). The switching rate is then plotted as a function of the tunneling current (I):

$$\text{Rate} = I^n$$

where n is the number of electrons involved in the process.[42] The results of these experiments are summarized in Figure 2B and demonstrate that when the bias is lower than threshold, activation of the switch occurs *via* a multi-electron process, whereas at and above the bias threshold activation occurs *via* a one-electron process. These two results allow us to calculate the electrical energy required to switch a single rotary switch: 99 ± 5 meV or 16 zJ.

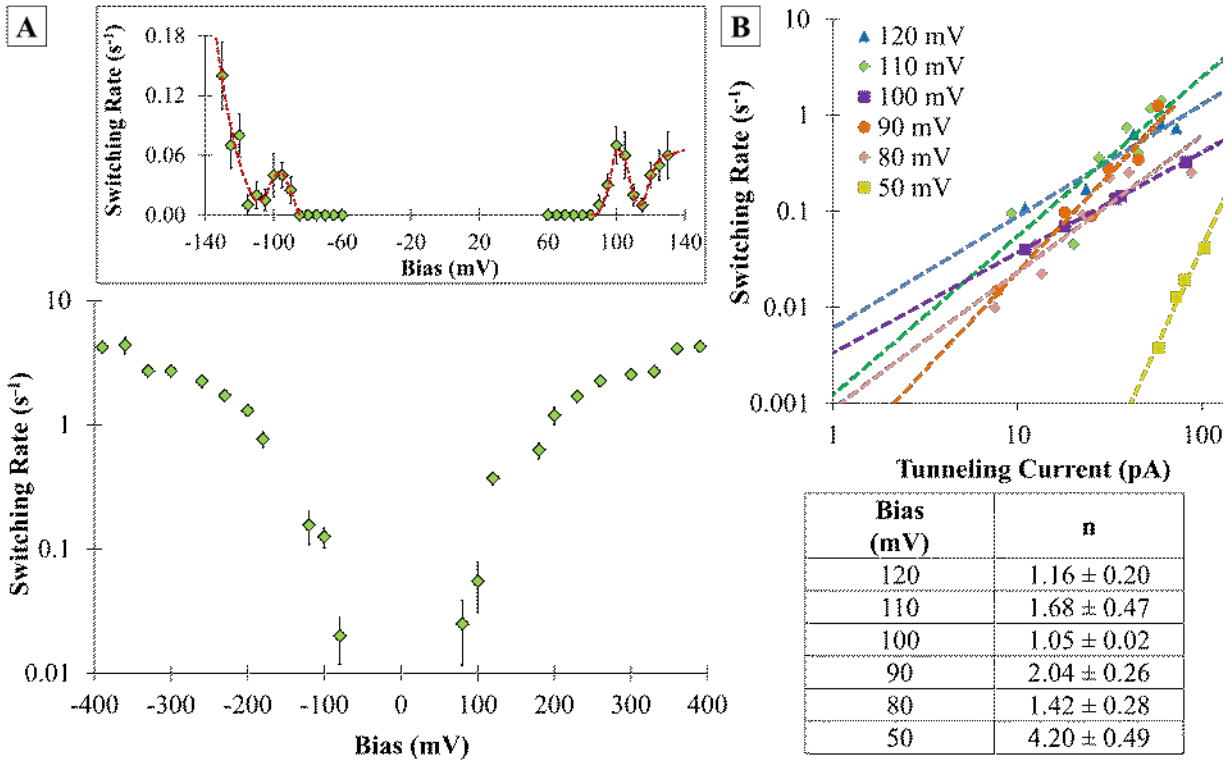

Bias (mV)	n
120	1.16 ± 0.20
110	1.68 ± 0.47
100	1.05 ± 0.02
90	2.04 ± 0.26
80	1.42 ± 0.28
50	4.20 ± 0.49

Fig. 2 (A) Action spectra for the 4-bromo-1-ethyl-2-fluorobenzene organometallic intermediate; plot of switching rate *vs.* bias. Inset: Action spectra for the −130 to 130 mV range at 5 pA. **(B)** Plot of switching rate *vs.* tunneling current at a range of biases. The slopes of the lines, **n**, gives the electron order of the process *i.e.* one *vs.* multiple electron induced switching.

In order to quantify the forces associated with switching of the individual molecular switches we first performed frequency shift *vs.* tip distance (Δf(z)) spectra with the nc-AFM. Figure 3A shows a series of Δf(z) traces taken above a rotary ethyl switch. At this low bias (20 mV) the switch is not activated and remains in the up position. Imaging before and after the Δf(z) measurements confirmed that these traces correspond to the up state of the switch. The shape of the Δf(z) trace indicates that as the AFM tip approaches the switch it transitions from an attractive to a repulsive regime. The Δf(z) trace minima is defined as z = 0. Figure 3B shows that when the same measurement is taken, but with an applied voltage (100 mV) that excites

switching of the ethyl rotor, one can clearly see two distinct Δf(z) traces corresponding to the switch in the up (lower traces) and down (upper traces) orientations. The vertical lines between the traces indicate fast stochastic switching between the two states as the switch is excited during the measurement. The effect of bias on the Δf(z) traces is small as seen in Figures S5 and S6 and within the error of the measurement.

Δf(z) spectra on the bare Cu surface were used to background subtract the contribution of the nc-AFM tip–Cu surface interaction from the tip–molecule–Cu surface interaction (Figure S1).[28,43] In Figure 3D, multiple Δf(z) traces (teal color) of the bare Cu surface were fitted to a polynomial (red), producing a fit with an average standard deviation for Δf across the range of z of ± 0.20 Hz. At zero applied voltage, with the rotor steady in the up position, these raw Δf(z) traces (green) are also shown in Figure 3D as well as their fitted function (blue); ± 0.21 Hz standard deviation. The black trace is the Cu background subtracted zero voltage trace and the Cu background is subtracted from all subsequent Δf(z) spectra presented; the effect of background subtraction on force calculation is shown in Figure S1. For spectra on the bare Cu surface, the minima in the Δf(z) trace occurs ~300 pm closer to the Cu surface than when the 2D molecular switch layer is present.[29] For the spectra seen in Figure 3B, the traces for the 'up' and 'down' rotors can be extrapolated (Figure 3 E) by methods explained in Figure S2. Δf(z) traces are vertically offset by values noted in Figures S5 A and S6 A such that Δf(z) = 0 at far tip distances.

Using the Sader and Javis method Δf(z) traces were converted to force(z) data (F(z)).[44] Figure 3F shows the F(z) traces for both the up and down configurations of the molecular switch. The negative values of the force indicate that both traces (corresponding to the switch up and down) are in the net attractive regime. In other words, the switch is most stable in the up position and

less stable in its down orientation. This result is verified by measurement of the lifetimes of the electrically excited switch in the up and down positions. Averaging ~800 switching events the total time spent in the up state (1772 s) is significantly higher than in the down state (1228 s) yielding an up/down lifetime ratio of 1.44:1.

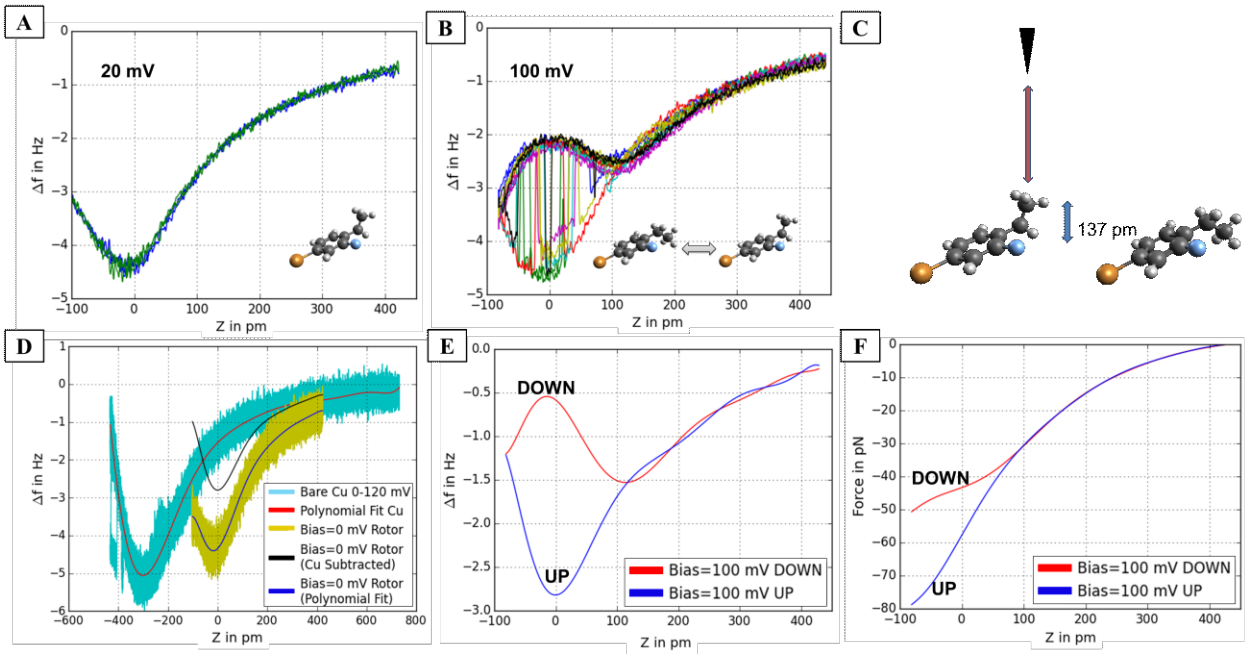

Fig. 3 (A) Frequency shift *versus* tip height (Δf(z)) spectra at 20 mV bias over the ethyl tail of a 4-bromo-1-ethyl-2-fluorobenzene organometallic intermediate in the 'up' position. **(B)** At a bias of 100 mV the ethyl rotor switches rapidly between 'up' and 'down' positions producing two distinct Δf(z) traces. **(C)** Side view schematic of the molecular switch in 'up' and 'down' orientations. **(D)** Multiple Δf(z) traces from bare Cu(111) (teal) are shown with a calculated polynomial fit (red). This Cu background is subtracted from the rotor switching data to isolate the contribution of the nc-AFM tip–molecule interaction. The traces for 0 mV bias over the ethyl rotor (green) are fitted (blue) and background subtracted to produce the final spectra (black). The minima of the background-subtracted, 0 mV bias trace was used to set z = 0 pm. **(E)** Distinct Δf(z) traces corresponding to 'up' and 'down' rotor positions from 100 mV spectra are derived from the

data shown in **(B)**, including Cu background subtraction. **(F)** Force *versus* tip height (F(z)) for 100 mV calculated by the Sader and Jarvis method[44] ($k \approx 1800$ N/m, $f_0 \approx 30800$ Hz, $Q \approx 18000$, $A_{osc} = 50\text{-}60$ pm).

Switching events with the highest tip-switch forces occur at the smallest tip-sample separations ($z \sim -80$ pm). Under these conditions the energy required to transition the switch from the up to down position, assuming that the force field is linear, can be calculated by multiplying the average of the forces the switch experiences in the up and down positions by the distance the switch moves normal to the surface. Specifically, at the closest tip distance, $z = -81.06$ pm in Figure 3F, the force exerted is $F_{down} = -50.68$pN and $F_{up} = -78.79$ pN. The hypothetical work the switch could perform on the AFM tip during the electrically induced switching event is then the integral of the force over the 137 pm distance between the rotor up and down positions, assuming that the force changes linearly between the up and down positions (see Figure S8). This number (137 pm) was verified by imaging individual molecular switches in their up and down positions in constant Δf mode (~ 140 pm) as shown in Figure S7. Integrating the force over this distance yields an energy of 8.9 zJ or 55 meV (Figure S8). The propagation of the ± 0.21 Hz standard deviation from the change in frequency shift spectra is visually presented in Figure S3 and propagates as about ± 12 pN spread in the determined force resulting in a ± 10 meV error in the switching energy calculation.

Comparing hypothetical work the tip could do on the cantilever (55 ± 10 meV) to the electrical energy required to induce a switching event (99 ± 5 meV) yields a hypothetical efficiency of ~55% for a single molecule switching event per inelastic tunneling electron induced switch. However, when considering the total electrical current during the measurement (5pA) and that at

a 100 mV excitation voltage yields switching rates ~0.05 Hz, only 1 in every ~$6x10^8$ tunneling electrons induces a switching event and this hypothetical efficiency drops to ~$1x10^{-7}$ %.

Furthermore, when examining the local regions around each single molecule switching event before and after a switch is electrically induced, we note that switching of one ethyl rotor induces switching of the ethyl rotor on its nearest neighboring molecule in a correlated manner (as seen in Figure 1F). As the ethyl switch under the STM tip is switched up, the neighboring ethyl switch simultaneously switches down and vice versa (Figure 4). Using the convention of labelling rotors in the 'up' position as 1 and the down position as 0,[34] these switching relationships are shown in Figure S4 with all possible combinations presented. The [1 0]↔[0 1] correlated switching events were observed 88% of the time suggesting that some of the extra mechanical energy imparted to the switch excited under the probe tip is transferred to the motion of a neighboring switch.

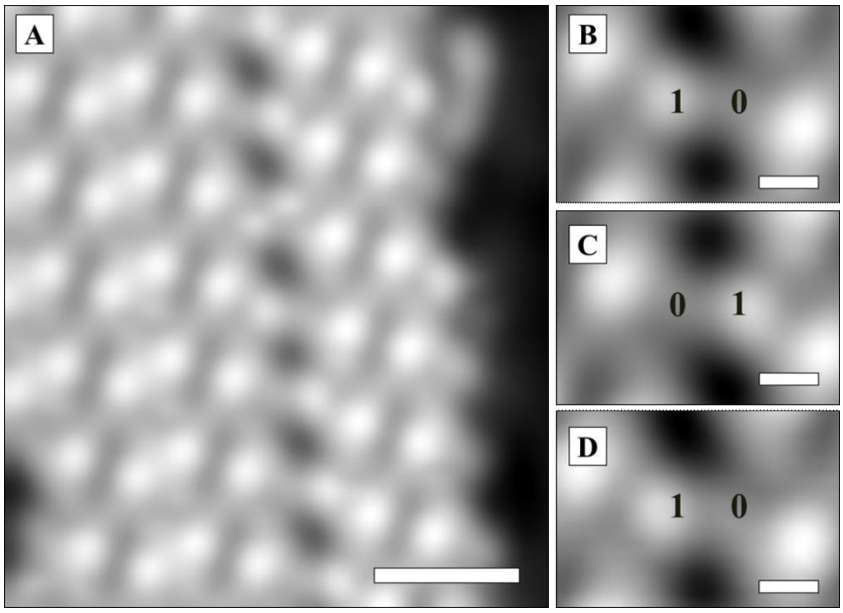

Fig. 4 5 K STM image of an active switching row in a 2D domain **(A)**. Zoom in images of pairs of active switches in the up (1) and down (0) positions in panels **B-D** show [1 0]↔[0 1] correlated switching

events that observed 88% of the time. Imaging conditions: −100 mV, 5 pA. Scale bar: **(A)** 2 nm, **(B - D)** 0.5 nm.

Conclusions

We report a system in which stochastic switching events can be driven resonantly by single tunneling electrons with an energy ~100 meV as measured by STM-based Action Spectroscopy and forces between the tip and switch simultaneously measured. Unlike a previous study in which electrically driven excitation of a layer of H_2 molecules induced oscillation of an AFM cantilever,[32] *individual* switching events could be detected due to the long lifetime of the up and down states of the individual single molecule switches. This enabled us to probe the forces between the AFM tip and the switch in both the up and down states of the switch. We find that the closer the AFM tip, the larger these forces. Measurement of the switch up/down lifetimes during tunneling electron excitation reveal that the up state of the switch is more stable, and AFM forces measurements confirm this. While the switching events are stochastic and no net work is done by the electrically excited switch on the AFM cantilever, the fact that we can measure the forces the switch experiences in the up and down positions allows us to calculate the amount of energy needed to transition the switch from up to down configuration by assuming that the force field is linear and normal to the surface. This energy is ~55 meV, which when compared to the 100 meV electron that induced the switching event, yields a hypothetical efficiency of 55% of the up to down switching event per *inelastic* tunneling electron. This number drops to ~$1x10^{-7}$ % when considering the total electrical energy associated with electron tunneling. While the switching of our system is random and no net work is done, this approach of quantifying energy input and the forces the molecule moves against should in fact be

somewhat general for electrically excited molecular machines and could be extended to optically driven devices if the energy input is quantized in the same way that inelastic electrical excitation is.

Experimental

LT-STM experiments at Tufts University were performed in an Omicron Nanotechnology GmbH low-temperature microscope, operating at a base pressure of $<1 \times 10^{-11}$ mbar. The cleaning cycle for the Cu(111) single crystal (MaTecK) consisted of multiple 1.5 keV Ar^+ bombardment and 1000 K anneal cycles. The cleanliness of the crystal was determined by STM prior to molecular deposition. 4-bromo-1-ethyl-2-fluorobenzene was acquired at 95% purity from Matrix Scientific and purified further *via* multiple freeze/pump/thaw cycles before depositing on Cu(111) at 5 K. The molecular ensembles were then converted into the 2D Ullmann coupling intermediate structures *via* annealing to ~260 K.

The non-contact Atomic Force Microscopy (nc-AFM) capability at Brookhaven National Laboratory's Center for Functional Nanomaterials was used for sample preparation, 5 K q-plus nc-AFM imaging and spectroscopy. The Cu(111) crystal was cleaned with repeated cycles of Ar+ ion sputtering and annealing. Small amounts of 4-bromo-1-ethyl-2-fluorobenzene were directly deposited on a Cu(111) sample at 5 K base temperature from a small transferable liquid source. Low coverages of the rotor were annealed to ~290 K while outside the cryostat shield. The sputtered PtIr tip was prepared by picking up a bromine atom left on the Cu(111) surface after the Ullman coupling reaction *via* close proximity scanning. The Br tip termination proved more effective than CO molecule termination when imaging the switching structures and in

spectroscopy measurements. Spectroscopy measurements were performed in consecutive bias sets with controlled approach and retraction of the tip over the same switching rotor. The location of the transition from attractive to repulsive in the frequency shift spectra of the rotor is consistent for the spectroscopy measurements presented in this manuscript at all biases. After background subtraction, this transition minima was set to z = 0 pm using the 0 V bias data set. Tuning fork sensors in the qPlus configuration had a resonance frequency of 30,800 Hz, spring constant of ~1,800 N/m, quality factor of 18,000 at 5 K and oscillation amplitude of 50 – 60 pm.

Acknowledgements

The project at Tufts (T.A.B., A.C.S., E.C.H.S.) was supported by NSF under grant CHE-1708397. A.M.L. was supported by NSF grant CHE-1764270. This research also involved personnel (P.Z. and D.S.) and resources of the Center for Functional Nanomaterials, which is a U.S. DOE Office of Science Facility, at Brookhaven National Laboratory under Contract No. DE-SC0012704.

Supporting Information Available

This section contains further information about background subtraction of frequency shift curves (Figure S1), deconvoluting switch up and down frequency shift curves (Figure S2), error determination (Figure S3), quantification of degree of correlated switching (Figure S4), effect of bias on frequency shift and force data (Figure S5, S6), displacement during a switching event (Figure S7), and calculation of the hypothetical work possible during an up to down switching event (Figure S8). This material is available free of charge at http://pubs.acs.org.

References

(1) Luo, Y.; Collier, C. P.; Jeppesen, J. O.; Nielsen, K. A.; DeIonno, E.; Ho, G.; Perkins, J.; Tseng, H. R.; Yamamoto, T.; Stoddart, J. F.; Heath, J. R. Two-Dimensional Molecular Electronics Circuits. *ChemPhysChem* **2002**, *3*, 519–525.

(2) Kelly, T. R.; Bowyer, M. C.; Bhaskar, K. V.; Bebbington, D.; Garcia, A.; Lang, F.; Kim, M. H.; Jette, M. P. A Molecular Brake. *J. Am. Chem. Soc.* **1994**, *116*, 3657–3658.

(3) Astumian, R. D. Design Principles for Brownian Molecular Machines: How to Swim in Molasses and Walk in a Hurricane. *Phys. Chem. Chem. Phys.* **2007**, *9*, 5067.

(4) Su, X.; Aprahamian, I. Switching around Two Axles: Controlling the Configuration and Conformation of a Hydrazone-Based Switch. *Org. Lett.* **2011**, *13*, 30–33.

(5) Haidekker, M. A.; Theodorakis, E. A. Molecular Rotors - Fluorescent Biosensors for Viscosity and Flow. *Org. Biomol. Chem.* **2007**, *5*, 1669–1678.

(6) Koumura, N.; Zijlstra, R. W. J.; van Delden, R. A.; Harada, N.; Feringa, B. L. Light-Driven Monodirectional Molecular Rotor. *Nature* **1999**, *401*, 152–155.

(7) Kelly, T. R.; Snapper, M. L. A Molecular Assembler. *Nature* **2017**, *549*, 336–337.

(8) Kudernac, T.; Ruangsupapichat, N.; Parschau, M.; Maciá, B.; Katsonis, N.; Harutyunyan, S. R.; Ernst, K.-H.; Feringa, B. L. Electrically Driven Directional Motion of a Four-Wheeled Molecule on a Metal Surface. *Nature* **2011**, *479*, 208–211.

(9) Seldenthuis, J. S.; Prins, F.; Thijssen, J. M.; Van Der Zant, H. S. J.; Jennings, N.; Lespérance, Y.; Seldenthuis, J. S.; Prins, F.; Thijssen, J. M.; Van Der Zant, H. S. J. An All-Electric Single-Molecule Motor. *ACS Nano* **2010**, *4*, 6681–6686.

(10) Kistemaker, J. C. M.; Štacko, P.; Roke, D.; Wolters, A. T.; Heideman, G. H.; Chang, M. C.; Van Der Meulen, P.; Visser, J.; Otten, E.; Feringa, B. L. Third-Generation Light-Driven Symmetric Molecular Motors. *J. Am. Chem. Soc.* **2017**, *139*, 9650–9661.

(11) Chaudhury, M. K.; Whitesides, G. M. How to Make Water Run Uphill. *Science* **1992**, *256*, 1539–1541.

(12) Eelkema, R.; Pollard, M. M.; Vicario, J.; Katsonis, N.; Ramon, B. S.; Bastiaansen, C. W. M.; Broer, D. J.; Feringa, B. L. Nanomotor Rotates Microscale Objects. *Nature* **2006**, *440*.

(13) Gross, L.; Mohn, F.; Moll, N.; Liljeroth, P.; Meyer, G. The Chemical Structure of a Molecule Resolved by Atomic Force Microscopy. *Science* **2009**, *325*, 1110–1114.

(14) Gross, L.; Mohn, F.; Moll, N.; Meyer, G.; Ebel, R.; Abdel-Mageed, W. M.; Jaspars, M. Organic Structure Determination Using Atomic-Resolution Scanning Probe Microscopy. *Nat. Chem.* **2010**, *2*, 821–825.

(15) Hapala, P.; Kichin, G.; Wagner, C.; Tautz, F. S.; Temirov, R.; Jelínek, P. Mechanism of High-Resolution STM/AFM Imaging with Functionalized Tips. *Phys. Rev. B - Condens. Matter Mater. Phys.* **2014**, *90*, 1–9.

(16) Riss, A.; Wickenburg, S.; Gorman, P.; Tan, L. Z.; Tsai, H.-Z.; de Oteyza, D. G.; Chen, Y.-C.; Bradley, A. J.; Ugeda, M. M.; Etkin, G.; Louie, S. G; Fischer, F. R; Crommie, M. F. Local Electronic and Chemical Structure of Oligo-Acetylene Derivatives Formed through Radical Cyclizations at a Surface. *Nano Lett.* **2014**, *14*, 2251–2255.

(17) Mönig, H.; Hermoso, D. R.; Díaz Arado, O.; Todorović, M.; Timmer, A.; Schüer, S.; Langewisch, G.; Pérez, R.; Fuchs, H. Submolecular Imaging by Noncontact Atomic Force

Microscopy with an Oxygen Atom Rigidly Connected to a Metallic Probe. *ACS Nano* **2016**, *10*, 1201–1209.

(18) Gross, L.; Mohn, F.; Moll, N.; Schuler, B.; Criado, A.; Guitian, E.; Pena, D.; Gourdon, A.; Meyer, G. Bond-Order Discrimination by Atomic Force Microscopy. *Science* **2012**, *337*, 1326–1329.

(19) de Oteyza, D. G.; Gorman, P.; Chen, Y.-C.; Wickenburg, S.; Riss, A.; Mowbray, D. J.; Etkin, G.; Pedramrazi, Z.; Tsai, H.-Z.; Rubio, A.; Crommie, M. F.; Fischer, F. R. Direct Imaging of Covalent Bond Structure in Single-Molecule Chemical Reactions. *Science* **2013**, *340*, 1434–1438.

(20) Riss, A.; Paz, A. P.; Wickenburg, S.; Tsai, H.-Z.; De Oteyza, D. G.; Bradley, A. J.; Ugeda, M. M.; Gorman, P.; Jung, H. S.; Crommie, M. F.; Rubio, A.; Fischer, F. R. Imaging Single-Molecule Reaction Intermediates Stabilized by Surface Dissipation and Entropy. *Nat. Chem.* **2016**, *8*, 678–683.

(21) Kocić, N.; Liu, X.; Chen, S.; Decurtins, S.; Krejčí, O.; Jelínek, P.; Repp, J.; Liu, S.-X. Control of Reactivity and Regioselectivity for On-Surface Dehydrogenative Aryl–Aryl Bond Formation. *J. Am. Chem. Soc.* **2016**, *138*, 5585–5593.

(22) Barth, C.; Foster, A. S.; Henry, C. R.; Shluger, A. L. Recent Trends in Surface Characterization and Chemistry with High-Resolution Scanning Force Methods. *Adv. Mater.* **2011**, *23*, 477–501.

(23) Ellner, M.; Pou, P.; Pérez, R. Molecular Identification, Bond Order Discrimination, and Apparent Intermolecular Features in Atomic Force Microscopy Studied with a Charge Density Based Method. *ACS Nano* **2019**, *13*, 786–795.

(24) Gross, L.; Mohn, F.; Liljeroth, P.; Repp, J.; Giessibl, F. J.; Meyer, G. Measuring the Charge State of an Adatom with Noncontact Atomic Force Microscopy. *Science* **2009**, *324*, 1428–1431.

(25) Gross, L. Recent Advances in Submolecular Resolution with Scanning Probe Microscopy. *Nat. Chem.* **2011**, *3*, 273–278.

(26) Ellner, M.; Pavliček, N.; Pou, P.; Schuler, B.; Moll, N.; Meyer, G.; Gross, L.; Peréz, R. The Electric Field of CO Tips and Its Relevance for Atomic Force Microscopy. *Nano Lett.* **2016**, *16*, 1974–1980.

(27) Gross, L.; Schuler, B.; Pavliček, N.; Fatayer, S.; Majzik, Z.; Moll, N.; Peña, D.; Meyer, G. Atomic Force Microscopy for Molecular Structure Elucidation. *Angewandte Chemie International Edition.* **2018**, *57*, 3888–3908.

(28) Ladenthin, J. N.; Frederiksen, T.; Persson, M.; Sharp, J. C.; Gawinkowski, S.; Waluk, J.; Kumagai, T. Force-Induced Tautomerization in a Single Molecule. *Nat. Chem.* **2016**, *8*, 935–940.

(29) Shiotari, A.; Odani, T.; Sugimoto, Y. Torque-Induced Change in Configuration of a Single NO Molecule on Cu(110). *Phys. Rev. Lett.* **2018**, *121*, 116101.

(30) Yamazaki, S.; Maeda, K.; Sugimoto, Y.; Abe, M.; Zobač, V.; Pou, P.; Rodrigo, L.; Mutombo, P.; Pérez, R.; Jelínek, P.; Morita, S. Interplay between Switching Driven by the Tunneling Current and Atomic Force of a Bistable Four-Atom Si Quantum Dot. *Nano Lett.* **2015**, *15*, 4356–4363.

(31) Pawlak, R.; Fremy, S.; Kawai, S.; Glatzel, T.; Fang, H.; Fendt, L. A.; Diederich, F.;

Meyer, E. Directed Rotations of Single Porphyrin Molecules Controlled by Localized Force Spectroscopy. *ACS Nano* **2012**, *6*, 6318–6324.

(32) Lotze, C.; Corso, M.; Franke, K. J.; von Oppen, F.; Pascual, J. I. Driving a Macroscopic Oscillator with the Stochastic Motion of a Hydrogen Molecule. *Science* **2012**, *338*, 779–782.

(33) Murphy, C. J.; Smith, Z. C.; Pronschinski, A.; Lewis, E. A.; Liriano, M. L.; Wong, C.; Ivimey, C. J.; Duffy, M.; Musial, W.; J. Therrien, A.; Thomas III, S. W.; Sykes, E. C. H. Ullmann Coupling Mediated Assembly of an Electrically Driven Altitudinal Molecular Rotor. *Phys. Chem. Chem. Phys.* **2015**, *17*, 31931–31937.

(34) Wasio, N. A.; Slough, D. P.; Smith, Z. C.; Ivimey, C. J.; Thomas III, S. W.; Lin, Y.-S.; Sykes, E. C. H. Correlated Rotational Switching in Two-Dimensional Self-Assembled Molecular Rotor Arrays. *Nat. Commun.* **2017**, *8*, 16057.

(35) Lewis, E. A.; Marcinkowski, M. D.; Murphy, C. J.; Liriano, M. L.; Therrien, A. J.; Pronschinske, A.; Sykes, E. C. H. Controlling Selectivity in the Ullmann Reaction on Cu(111). *Chem. Commun.* **2017**, *53*, 7816–7819.

(36) Balema, T. A.; Ulumuddin, N.; Murphy, C. J.; Slough, D. P.; Smith, Z. C.; Hannagan, R. T.; Wasio, N. A.; Larson, A. M.; Patel, D. A.; Groden, K.; McEwen, J.-S.; Lin, Y.-S.; Sykes, E.C.H. Controlling Molecular Switching *via* Chemical Functionality: Ethyl *vs* Methoxy Rotors. *J. Phys. Chem. C* **2019**, *123*, 23738–23746.

(37) Zint, S.; Ebeling, D.; Schlöder, T.; Ahles, S.; Mollenhauer, D.; Wegner, H. A.; Schirmeisen, A. Imaging Successive Intermediate States of the On-Surface Ullmann Reaction on Cu(111): Role of the Metal Coordination. *ACS Nano* **2017**, *11*, 4183–4190.

(38) Nguyen, M. T.; Pignedoli, C. A.; Passerone, D. An *Ab Initio* Insight into the Cu(111)-Mediated Ullmann Reaction. *Phys. Chem. Chem. Phys.* **2011**, *13*, 154–160.

(39) Yang, M. X.; Xi, M.; Yuan, H.; Bent, B. E.; Stevens, P.; White, J. M. NEXAFS Studies of Halobenzenes and Phenyl Groups on Cu(111). *Surf. Sci.* **1995**, *341*, 9–18.

(40) Xi, M.; Bent, B. E. Iodobenzene on Cu(111): Formation and Coupling of Adsorbed Phenyl Groups. *Surf. Sci.* **1992**, *278*, 19–32.

(41) Kim, Y.; Motobayashi, K.; Frederiksen, T.; Ueba, H.; Kawai, M. Action Spectroscopy for Single-Molecule Reactions - Experiments and Theory. *Prog. Surf. Sci.* **2015**, *90*, 85–143.

(42) Stipe, B. C; Rezaei, M. A; Ho, W. Single-Molecule Vibrational Spectroscopy and Microscopy. *Science* **1998**, *280*, 1732–1735.

(43) Albrecht, F.; Bischoff, F.; Auwärter, W.; Barth, J. V.; Repp, J. Direct Identification and Determination of Conformational Response in Adsorbed Individual Nonplanar Molecular Species Using Noncontact Atomic Force Microscopy. *Nano Lett.* **2016**, *16*, 7703–7709.

(44) Sader, J. E.; Jarvis, S. P. Accurate Formulas for Interaction Force and Energy in Frequency Modulation Force Spectroscopy. *Appl. Phys. Lett.* **2004**, *84*, 1801–1803.

TOC Figure